Propulsion Performance Investigation of Bio-inspired Nano Rotor Base on Fluid-Structure Interaction

Z. Liu*, P. Che, B. Li, S. Zhao, T. Dang, C. Bu
School of Aerospace Engineering, State Key Laboratory for Strength and Vibration of Mechanical Structures, Xi'an Jiaotong University, No.28 Xianning West Road, Xi'an, Shaanxi 710049, China

ABSTRACT

The bio-inspired blade motion is introduced to improve the propulsive performance of nano rotor at an ultra-low Reynolds number. However, the complex flow interacts with the flexible composite blade structure resulting in the change of nano rotor propulsion performance and the vibration of blade structure. In this paper, a composite nano rotor with blade-pitch motion is investigated computationally with a computational solvers based on fluid-structure interaction. The finite element model for composite rotor is created and verified with a non-contact modal test. It is found that the simulation results matched well with the experimental results. Successively, the propulsive performance of a rigid nano rotor is studied. The propulsive performance of the nano rotor is analysed at different bio-inspired pitch frequency. Results show that the figure of merit of the bio-inspired pitch rotor increases because of the bio-inspired blade pitch motion. And it is also found that the improvement of the propulsive performance of the nano rotor varies with the pitch frequency. The propulsive performance of the flexible bio-inspired nano rotor is also studied with by using fluid-structure interaction method. It is found that the computational results for flexible nano rotor are lower than that for rigid nano rotor. It is evident that it is necessary to consider the flexibility of the composite nano rotor when investigating the propulsion performance of bio-inspired nano rotor. And the response of blade structure is also studied. Structural dynamic analysis shows that the blade structure vibrates with small amplitude. And two peak values are found at the rotation frequency and the fundamental frequency of the nano rotor structure.

1 INTRODUCTION

Rotary-wing Nano Air Vehicle (NAV) is a kind of small unmanned air vehicle powered with one or several rotors. NAV which has a maximum size of 7.5 cm and a minimum payload of 2 g is able to enter buildings, penetrate narrow entries, and transmit data without being detected at a low speed [1, 2, 3]. The nano rotor operating at a Reynolds number of lower than 20,000 is the main propulsion component of the rotary-wing NAV. At such a low Reynolds number, the aerodynamic performance of the nano rotor degrades and the figure of merit (FM) of the nano rotor drops as a result [4]. Liu et al. [5] measure the hovering performance of the propeller U-80 with diameter of 8 cm. Results show that the FM of the propeller is about 0.45 which is far lower than that of the full-scale helicopter. Therefore, how to improve the propulsion performance of the nano rotor is

*contact email: liuz@mail.xjtu.edu.cn

an important issue for the NAV design. However, the traditional method using the steady aerodynamic theory to optimize the propeller can only improve the propulsion performance limitedly.

Flying Insect whose size is comparable to NAV has a high aerodynamic efficiency. Lots of research shows that the unsteady mechanics induced by the flapping wing is the reason. The high-lift unsteady aerodynamic mechanisms include the clap-Fling, delayed stalled, rotational circulation and wake capture [6-8]. Some research is carried out by applying the high-lift unsteady mechanisms on the rotor to improve its aerodynamic efficiency [9, 10]. Fitchett [10] studies experimentally a conventional rotor, a rotor with powered blade flapping, and a freely rotating rotor with powered blade flapping. Results show that the maximum thrust increases by up to 15% and the torque required is reduced by up to 30% with conventional rotation plus powered blade flapping at up to 8 per rotor revolution (/Rev) at a reduced frequency of 0.6. Great enhancement can be found due to the blade flapping motion, but flapping motion requires more power to overcome the inertial force and aerodynamic load on the rotor blade due to the high rotational velocity. Koratkar [11] tests the blade pitch motion of a 22cm-diameter two bladed mciro rotor system featuring piezoelectricaly actuated controllable twist rotor blades to investigate the improvement in aerodynamic performance of micros rotors. The blade is motivated by two piezo-electrical beams allowing of changing the collective angle of blade. A 2.3° blade unsteady tip twist deformation is found resulting in an improvement of up to 11% at 24° rotor collective pitch. Results show that the blade pitch motion has an impact on the thrust once the stall onsets at the airfoil section of rotor blades. However, the crossing piezo-electrical beams limit the amplitude of oscillation. Ellington [12] finds that the attached LEV is one of the reasons of high lift for flying animals. The attached LEV induces the higher stall angle and delays the stall of the wing. As the nano rotor blade size is comparable to that of flying insect, the bio-inspired blade motion can be introduced to improve the aerodynamic performance of nano rotor. The blade pitch motion can be employed along the longitudinal axis of blade to keep the leading edge vortex.

As the weight of NAV is limited, it is required that the nano rotor is light and thin enough [13]. Carbon composite laminate is used to fabricate the rotor blade. Because the composite blade is thin and light, the blade is flexible [14]. Due to the unsteady aerodynamic force, centrifugal force and the gravity, the flexible blade suffers the deformation and vibration which influences the flow field of nano rotor. The coupling between structure and fluid has an effect on the propulsive performance of the bio-inspired rotor. Therefore, the blade cannot be treated as a rigid body but a flexible one. The fluid-structure interaction shall be taken into account when studying the propulsive performance of the bio-inspired nano rotor. The research on the nano rotor with FSI method is scarcely reported. But the full-scale rotor is well studied based on FSI using experiment or numerical method in recent years [15-19]. When we study the propulsive performance of the bio-inspired nano rotor with FSI method, the first step is to obtain an accurate finite-element structural model of composite nano rotor. However, the fabrication error and the difference of material parameters will introduce nondeterminacy in the structural model. The modal experiment is usually carried out to validate the structural model. Yang [20], Luo [21] and Mohammad [22] adopted hammer to excite rotors and measured structural response by means of acceleration sensors onto structure surface. However, because traditional contact modal test methods will introduce additional mass and change the boundary conditions, they are not suitable for thin, small and flexible nano

rotor. Non-contact modal test methods, for instance acoustic excitation and laser vibrometer, are widely used by simple and large size structures [23, 24]. So, a non-contact modal test method is necessary. Since there are three different motions for the bio-inspired rotor, i.e. the rotation around the hub, the bio-inspired pitch motion, and the deformation due to the aerodynamic force, centrifugal force and the gravity force, the method to describe the coupling motions is another important issue for the study of the bio-inspired rotor. Sliding mesh method and Multiple References Frame method (MRF) are widely used to study the rotating rotor. Sliding mesh method which is suitable for the research on the fine flow field of rotor requires more computational resource than MRF. As we focus more on the propulsive performance of the bio-inspired nano rotor in this research, MRF is used to describe both the rotation motion and the bio-inspired motion. The deformation of the structure is related to local change of solid surface, so the sliding mesh method and MRF fail to describe it. Therefore, the deforming grid method is used. To study the bio-inspired rotor with the FSI method, a weak coupling method is used by transfer data at the interface of the structural model and the fluid model for the bio-inspired nano rotor. The interpolation method for FSI during the simulation is important [25-26]. RBF method constructs a Radial Basis Function and uses it to obtain the unknown parameters at the interface. It is simple and can be used for complex mesh. Therefore, RBF interpolation method is a useful method for this study.

In summary, the bio-inspired unsteady mechanisms are mainly used on flapping wing NAV and scarcely on rotary-wing NAV. And the propulsive performance of the bio-inspired nano rotor is scarcely studied with FSI method. In this study, the bio-inspired unsteady mechanism is introduced to improve the aerodynamic performance of the nano rotor. A non-contact modal test experimental platform is built based on sound excitation instrument and laser vibrometer and a modal test of the nano rotor is carried out. Successively, the finite element model of the nano rotor is established and verified with the modal test. Then propulsive performance of the bio-inspired nano rotor is analysed at different bio-inspired pitch frequency and the response of the blade structure is also analysed with the fluid-structure interaction method.

2 COMPUTATIONAL METHODOLOGIES AND EXPERIMENTAL PLATFORM

2.1 Governing Equations

The blade tip velocity of the nano rotor is lower than 0.1 Mach. The low-speed performance is extremely poor for compressible NS equations because of stiffness of governing equations which is caused by the small ratio of the convective speed to the speed of sound. Therefore, the preconditioning techniques are introduced to eliminate the disparity between the particle and acoustic wave speeds at low speed. The preconditioned governing equations can be rewritten as follows [27].

$$\Gamma\frac{\partial}{\partial t}\iiint_V q dV+\oiint_{\partial V}(E-E_V-u_g Q)\cdot n_x dS+\oiint_{\partial V}(F-F_V-v_g Q)\cdot n_y dS+\oiint_{\partial V}(G-G_V-w_g Q)\cdot n_z dS=0 \quad (1)$$

Here, Γ is the preconditioning matrix, Q is vector of primitive flow variables. $\vec{F}$ and $\vec{F}_v$ termed vector of convective fluxes are related to the convective transport of quantities in the fluid. $\vec{F}_v$ termed vector of viscous fluxes contain the viscous stresses τ_{ij}. In the formula, $\vec{U}$ and $\vec{U}_g$ are the velocity component and moving grid velocity component. The equations were solved with finite

volume method and Roe's flux scheme was employed.

2.2 Structural Dynamic Equations

The finite element method (FEM) formulations can be established on the basis of the finite deformation theory. Assumed that the composite material of nano rotor is linearly elastic and orthotropic, By taking into account the three loads, corresponding kinetic equation of nano rotor can be written as follows [28].

$$[\boldsymbol{M}]\{\ddot{\boldsymbol{x}}\}+[\boldsymbol{C}]\{\dot{\boldsymbol{x}}\}+[\boldsymbol{K}]\{\boldsymbol{x}\}=\{\boldsymbol{F}_{ce}\}+\{\boldsymbol{F}_{g}\}+\{\boldsymbol{F}_{h}\} \quad (2)$$

where $\ddot{x}$ represents node acceleration, x is node displacement, M is mass matrix, C is damping matrix, K is stiffness matrix ; F_{ce}, F_g and F_h are centrifugal force, gravity and aerodynamic force, respectively.

2.3 Fluids-Structure Interaction Method

A loose-coupling method is used in the FSI simulation. Because the FEM mesh is different from the CFD mesh, the data shall be transferred at the interface. The RBF method is used in this study. The deforming grid method is used in the CFD solver. Time-marching method is a sequential coupling method. The aerodynamic force is firstly calculated with CFD solver. Then the aerodynamic force together with gravity and centrifugal force will be interpolated on the FEM mesh with which the structural dynamic response can be calculated with the FEM solver. The node displacement will be transferred to the CFD solver and the mesh will be updated with displacement. Then the flow field will be calculated again and the aerodynamic force will be obtained. The solver will keep on repeat the above calculation.

2.4 Bio-inspired Pitch Motion

Figure 1 shows a schematic of the motion for the nano rotor. Two blades rotate around the central axis and pitch around the 1/4 chord along the blade. To describe the motion of the nano rotor, two coordinate systems are introduced. The fist coordinate system $O-XYZ$ is an inertial coordinate system which keeps motionless and the other coordinate system $O'-X'Y'Z'$ is a comoving coordinate which rotates with the rotor blade. The origin of the coordinate systems locate on the centre of the 1/4 chord along the blade. The pitch angle, the flapping angle and the roll angle are defined as θ, ϕ and γ. At the beginning, the $O'-X'Y'Z'$ concides with $O-XYZ$. But $O'-X'Y'Z'$ changes with the rotation and pitch for the blade. The transform matrix between the $O-XYZ$ and $O'-X'Y'Z'$ can be write as

$$\begin{pmatrix} x \\ y \\ z \end{pmatrix} = \begin{pmatrix} -\sin\theta\cos\gamma & \sin\theta\sin\gamma & \cos\theta \\ \cos\theta\cos\gamma & -\cos\theta\sin\gamma & \sin\theta \\ \sin\gamma & \cos\gamma & -\sin\theta \end{pmatrix} \begin{pmatrix} x' \\ y' \\ z' \end{pmatrix} \quad (3)$$

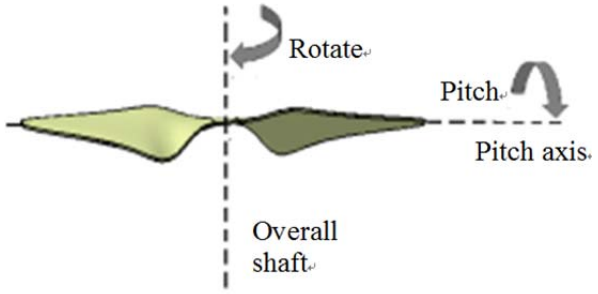

Figure 1 - Schematic of rotor pitch motion.

When inserting a table, you can choose the appropriate style - Table 1 below is an example. Put the caption under the table.

The rotational speed of the nano rotor is 6500RPM. Then the pitch motion of the blade is defined as a sine function

$$\theta(t)=\theta_0\cdot\sin(2\pi f_p t)+\theta_{hias} \quad (4)$$

where $\theta(t)$ is the pitch angle varying with the time. θ_0 is the amplitude of the pitch motion which is 5° in this study. f_p is the pitch frequency. θ_{bias} is the initial pitch angle which is zero.

2.5 Modal test Experimental Setup

Traditional contact-type modal test method cannot be adopted because extra mass and stiffness will be introduced. In this study, a non-contact modal experiment platform for nano rotor was established based on sound excitation instrument and laser vibrometer as shown in Figure 2. This test platform include supporter of the nano rotor, sound excitation instrument and laser vibrometer. The full frequency speaker was excited by broadband white noise signal, which was also inputted into the Polytec laser vibrometer system as a reference signal. The SPL of the sound generated is from 100 to 110dB. A two-dimensional modal test was performed for the rotor. Seventy to eighty laser scanning points were set on the surface of nano rotor and their vibration displacements were measured by virtue of Doppler Effect. All the measured signals were processed to filter the useless signals and reduce the noise so as to ultimately obtain the accurate frequency spectrum and vibration modes of nano rotor.

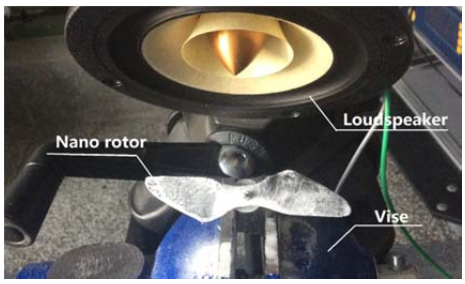

Figure 2 - Modal test bench for nano rotor.

3 RESULTS AND DISCUSSION

3.1 Dynamic Characteristics Analysis of Nano Rotor

The nano rotor using for modal test was laminated by 6 layers unidirectional fibre composite and the stacking sequence in Fig. 4 (a) was [0/90/0/90/0/90]. Every layer thickness was 0.85mm and the total thickness of rotor was 0.51mm. The platform adopted the method of acoustic excitation and laser vibration measurement technology. Five natural frequencies and vibration modes were obtained.

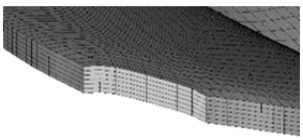

Figure 3 - FE model of nano rotor.

When comparing the experimental results and computational results, it is found that the two groups of vibration modes are extremely similar in flapping, bending and torsion according to the similar vibration modes. The corresponding natural frequencies are also compared in Table 1. It is found that the relative errors for them are lower than 4%. The first two natural frequencies are also comparable to the rotating frequency of the nano rotor, which shall be paid more attention to during the design of the NAV to avoid the resonance. Because the maximum relative error of simulation is lower than 4% and the minimum relative error is even lower than 1%, the finite element model is thought to be capable of reflecting the main structural feature of nano rotor.

Order	Natural frequency of experiment /Hz	Natural frequency of simulation /Hz	Relative Error/%
1	303.10	294.45	2.84
2	310.90	304.77	1.96
3	1131.30	1176.1	3.96
4	2743.70	2816.8	2.66
5	3181.30	3202.4	0.6

Table 1 - Comparison of natural frequencies between experiment and computation.

3.2 Propulsive performance of bio-inspired Rigid Nano Rotor

MRF is used to describe the rotation and the pitch motion in this study. The flow field is composed of a static block, a rotation block and a pitch block as shown in Figure 4. The pitch block which contains two blades is a cylinder with a radius of 0.5 R and a height of 1.2R. The rotation block located outside of the pitch block is also a cylinder with a radius of 2.4R and a height of 1.6R. The static block is a cone with a upper radius of 6R and a lower radius of 8R. The structure mesh is is used for static block and the unstructured mesh is used for both the rotation block and the pitch block. The total number of the mesh is about 8 million.

The rotational speed of nano rotor is 6500 RPM. Three cases are calculated including case 1 in which there is no pitch motion, case 2 in which the pitch frequency $f_p = f_0$ and the pitch case 3 with frequency $f_p = 2f_0$. The simulation is carried out on a HP station with 64GB RM and 40 cores.

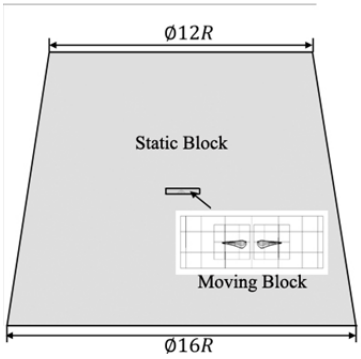

(a) Moving block and static block.

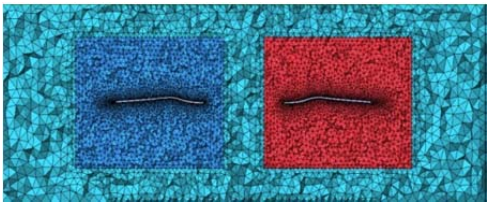

(b) Mesh section.

Figure 4 - Computation Zone and mesh of rotor for CFD.

Figure 5 shows the thrust and the torque of the nano rotor varying with the azimuth. It is found that the curves of thrust and the torque resemble sine or cosine function. And the periods of the curves corresponds with that of the pitching motion. The frequency of the curve increases with the pitching frequency. The amplitude of the thrust and torque increases with the frequency as well. For the non-pitching case, the value of the thrust and the torque keeps as an equilibrium value.

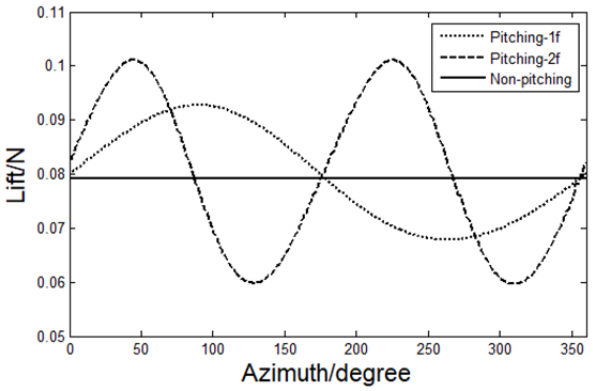

(a) Lift.

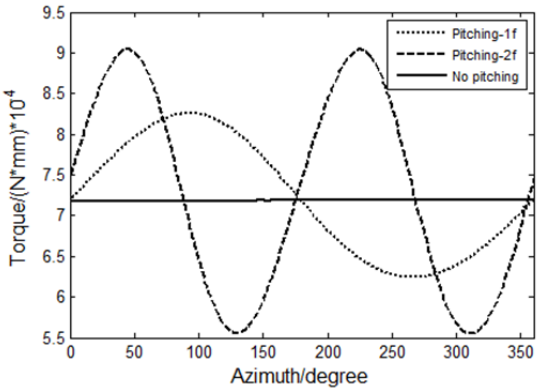

(b) Torque

Figure 5 - Lift and torque curves of pitching rigid rotor in one cycle

The average value in a cycle for the thrust coefficient, the torque coefficient and the figure of merit are summarized in table 2. It is found that

the thrust coefficient increase with the pitching frequency. The non-pitching case obtains the minimum FM. And the maximum FM is achieved by the pitching case with high pitching frequency. It is indicated that the propulsive performance of the nano rotor is improved with the bio-inspired pitching motion.

Cases	Thrust coefficient	Torque coefficient	FM
Case 1	0.0450	0.0109	0.625
Case 2	0.0454	0.0108	0.633
Case 3	0.0455	0.0108	0.635

Table 2 – Propulsive performance for different cases.

Figure 6 shows the pressure coefficient varying with chord at the sections of r/R=68%, 80% and 96% along the blade for the three case. It is found that the difference of the pressure coefficient at the suction surface and press surface increases with the pitching angle and pitching frequency. At the high pitching angle, the pressure coefficient at the press surface for case 2 and case 3 is higher than that for case 1. The variation of the pressure coefficient with the pitching angle indicates that the pitching motion changes the velocity of the LEV shedding. At high pitching angle, LEV attaches on the surface which induces high pressure coefficient difference. However, the pressure coefficient curve varies from the other at the section of r/R=96% due to the blade tip vortex.

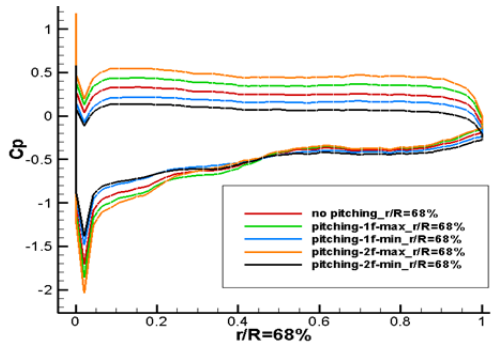

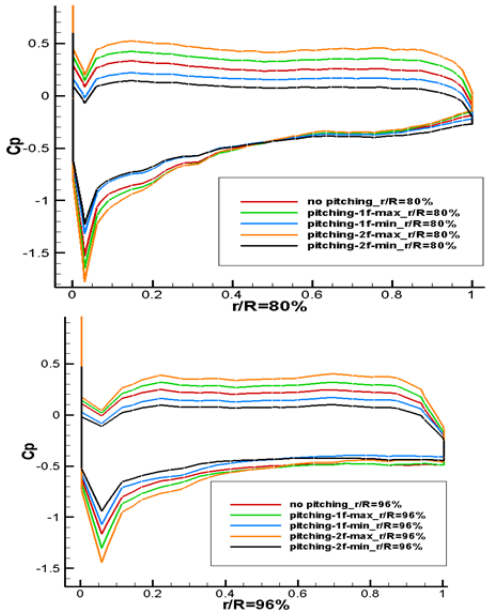

Figure 6 - Pressure coefficient comparison at different blade sections for different cases.

Figure 7 shows iso-surface of the magnitude of vorticity. At high pitching angle, the biggest iso-surface is shown which indicates that the vorticity is the strongest. The pitching motion influences the vorticity and propulsive performance of the nano rotor as a result.

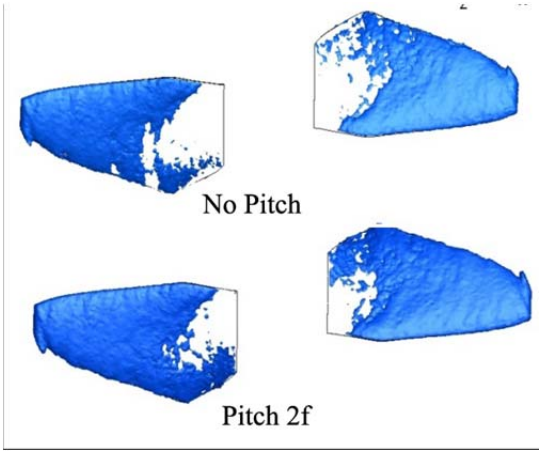

Figure 7 – Iso-surface of vorticity for the non-pitch nano rotor and the pitching nano rotor.

3.3 Propulsive performance of bio-inspired flexible Nano Rotor

The bio-inspired flexible nano rotor with pitching frequency of $f_p = 2 f_0$ is also studied with FSI

method. Figure 8 shows the thrust and the e torque varying with azimuth in one cycle for both flexible rotor and rigid rotor. It is found that the thrust of the flexible nano rotor is slightly lower than that of the rigid one. However, the torque of the flexible nano rotor approximates that of the rigid one. The average thrust coefficient and torque coefficient of both flexible Nano rotor and rigid nano rotor are also shown in Table 3. Results show that both the thrust coefficient and torque coefficient are lower than that of the rigid nano rotor. As the more drop can be found in the thrust coefficient, the FM of flexible is lower than that of rigid one. It is indicated that the propulsive performance of nano rotor degrades with the flexibility of nano rotor and it is necessary to carry out the FSI method when we investigate the propulsive performance of the nano rotor.

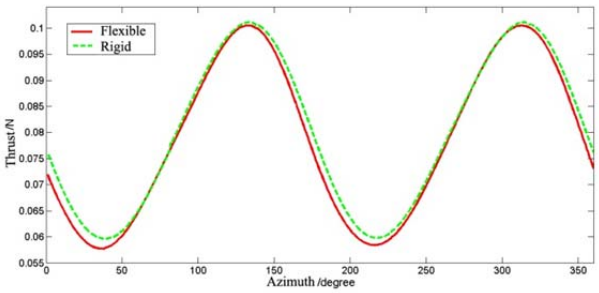

(a)

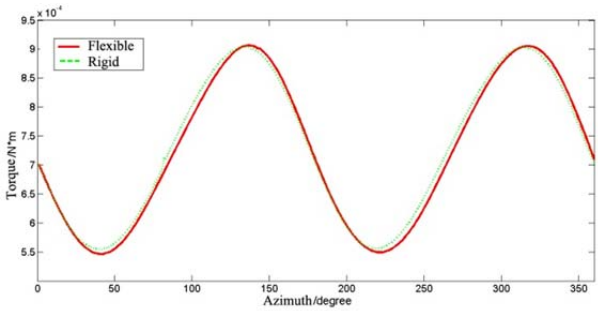

(b)

Figure 8 – Thrust and torque varying with the azimuth for both flexible and rigid nano rotor.

Cases	Thrust coefficient	Torque coefficient	FM
Flexible	0.0446	0.0106	0.628
Rigid	0.0455	0.0108	0.635

Table 3 – Propulsive performance for flexible and rigid nano rotor.

Figure 9 shows the pressure coefficient at different blade stations i.e. r/R=50% and 96% for both flexible and rigid bio-inspired nano rotor when the rotor achieves the maximum thrust coefficient. It is found that the curve of the pressure coefficient for the flexible nano rotor nearly locates inside of that for the rigid nano rotor at all the blade stations except at r/R=96%. The deformation of the nano rotor at the blade tip is large which might induces the difference.

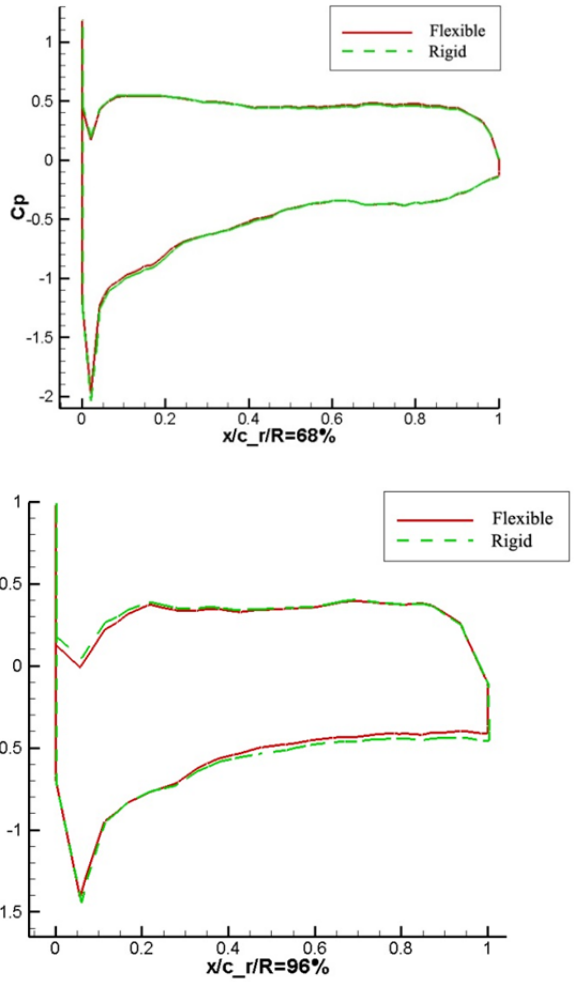

Figure 9 – Thrust and torque varying with the azimuth for both flexible and rigid nano rotor.

3.4 Structural response of bio-inspired flexible Nano Rotor

Figure 10 shows Displacement and stress contour of the nano rotor. At the beginning, the maximum displacement vibrates irregularly. The maximum amplitude is as high as 0.2 mm. Then, it begins to vibrate regularly. Results show that the maximum of the displacement is about 0.118mm at the blade tip. The maximum stress is found at the blade root. The two blades tilt due to the aerodynamic force.

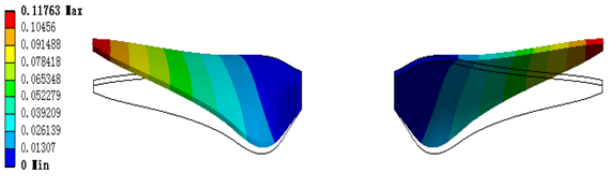

(a) Displacement Contour

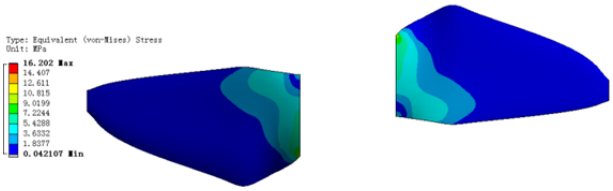

(b) Stress contour

Figure 10 - Displacement and stress contour of the nano rotor.

The amplitude spectrum of displacement at the blade tip is shown in Figure 11. There are two peak values at frequency of 211.9 Hz and 605.46Hz. When comparing with the modal test results, it is found that the first frequency is close to the rotational frequency. And the second frequency is close to the fundamental frequency of the nano rotor.

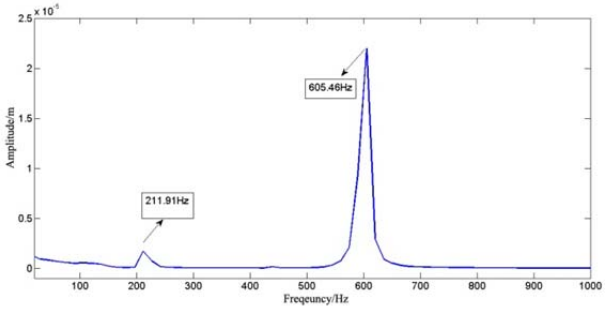

Figure 11 – Amplitude spectrum of displacement

6 CONCLUSION

In this paper, the bio-inspired composite nano rotor is studied with FSI method. Blade pitch motion is introduced to improve the propulsive performance of the nano rotor performance. The bio-inspired blade motion is introduced to improve the propulsive performance of nano rotor at an ultra-low Reynolds number. A non-contact modal experimental platform is firstly established using sound excitation instrument and laser vibrometer. The structural characteristics of the composite nano rotor are measured. It is found that the natural frequencies are very close for the first two orders. The finite element model of composite rotor is created accordingly. The modal is studied computationally with FEM solver. It is found that the simulation results matched well with the experimental results which verified the correctness of the finite element model. The CFD model is established and the propulsive performance of the rigid bio-inspired nano rotor motion is studied at different pitch frequencies. Results show that the thrust and torque for the bio-inspired pitching rotor are higher than those for the rotor without bio-inspired motion and the propulsive performance for the nano rotor with bio-inspired pitching frequency of two times of that rotation frequency is higher than that with only one times pitching frequency. It is evident that the improvement enhanced with the increase of the pitching frequency. The flexible bio-inspired nano rotor is then investigated with FSI method. The results show that the propulsive performance

of the flexible nano rotor is lower than that of the rigid nano rotor. It is evident that it is necessary to consider the flexibility of the composite nano rotor when investigating the propulsion performance of bio-inspired nano rotor. Then the response of blade structure is also analysed. Results show that the blade structure vibrates at small amplitude. In general, it is found that the bio-inspired pitching motion can improve the performance of nano rotor. In the future, the experiment will carry out to further verify the c

ACKNOWLEDGEMENTS

Authors are grateful for the support from the National Natural Science Foundation of China through grant numbers 11772252 and 11302164. The authors also acknowledge the support of K. C. Wong Education Foundation.

REFERENCES

[1] C. De Wagter, S. Tijmons, B.D.W. Remes, and G.C.H.E. de Croon. Autonomous flight of a 20-gram flapping wing mav with a 4-gram onboard stereo vision system. In IEEE Conference on Robotics and Automation (ICRA), 2014.

[2] S. Nolfi. Power and the limits of reactive agents. Neurocomputing, 42(1–4):119–145, 2002.

[3] C.M. Bishop. Pattern recognition and machine learning. Springer Science and Business Media, LLC, New York, NY, 2006.

[1] H. Todd, ,M. Christopher, and T. Richmon, The DARPA Nano Air Vehicle Program. In 50th AIAA Aerospace Sciences Meeting including the New Horizons Forum and Aerospace Exposition, 2012.

[2] S. Sato, M. Drela, J.H. Lang, and D.M. Otten. Design and characterization of hover nano air vehicle propulsion system. In 27th AIAA Applied Aerodynamics Conference, 2009.

[3] H. Youngren, C. Kroninger, M. Chang, and S. Jameson. Low Reynolds number testing of the AG38 airfoil for the SAMARAI nano air vehicle. In 46th AIAA Aerospace Sciences Meeting and Exhibit, 2008.

[4] Z. Liu, A. Roberto, J.M. Moschetta, and C. Thipyopas. Experimental and computational evaluation of small micro coaxial rotor in hover. Journal of Aircraft 48(1):220–229., 2011.

[5] Z. Liu, J.M. Moschetta, N. Chapman, R. Barenes, and M. Xu. Design of Test Benches for the Hovering Performance of Nano-Rotors. International Journal of Micro Air Vehicles, vol. 2(1):117-32, 2010.

[6] R. J. Wootton. The Mechanical Design of Insect Wings. Scientific American, 263:114-120, 1990.

[7] N. Phillips, K. Knowles. Effect of flapping kinematics on the mean lift of an insect-like flapping wing. Proceedings of the Institution of Mechanical Engineers Part G Journal of Aerospace Engineering, 225:723-736, 2011.

[8] W. Shyy, H. Aono, S. K. Chimakurthi, et al. Recent progress in flapping wing aerodynamics and aeroelasticity. Progress in Aerospace Sciences, 46(7):284-327, 2010.

[9] S. Guo, D. Li, J. Wu. Theoretical and experimental study of a piezoelectric flapping wing rotor for micro aerial vehicle. Aerospace Science & Technology, 23(1):429-438, 2012.

[10]B. Fitchett Development and Investigation of a Flapping Rotor for Micro Air Vehicles. Dissertations & Theses - Gradworks, 2007.

[11] N.A. Koratkar, and I. Chopra. Open-loop hover testing of a smart rotor model. AIAA Journal, Vol. 40(8): 1495-1502, 2002.

[12] C.P. Ellington. The novel aerodynamics of insect flight: applications to micro-air vehicles. Journal of Experimental Biology, 202(23):3439-3448, 1999.

[13] N. Tsuzuki, S. Sato, and T. Abe. Design guidelines of rotary wings in hover for insect-scale Micro Air Vehicle applications. Journal of Aircraft, vol. 44(1): 252-263, 2002.

[14] Z. Liu. Design and aero-propulsive analysis of a nano air vehicle. Ph. D., L'INSTITUT SUPÉRIEUR DE L'AÉRONAUTIQUE ET DE L'ESPACE, Toulouse, 2011.

[15] F. Bohorquez, D.J.Pines, and P.D. Samuel. Small rotor design optimization using blade element momentum theory and hover tests. Journal of Aircraft, vol. 47(1): 268-283, 2010.

[16] A. Smedresman, D. Yeo, and W. Shyy. Design, fabrication, analysis, and testing of a micro air vehicle propeller. In 29th AIAA Applied Aeroydnamics Conference, 2011.

[17] P. Singh, and C. Venkatesan, , Experimental Performance Evaluation of Coaxial Rotors for a Micro Aerial Vehicle, Journal of Aircraft, vol. 50(5): 1465-1480, 2013,.

[18] M. I. Kellogg, and B. W. J. Parametric design study of the thickness of airfoils at Reynolds numbers from 60,000 to 150,000. In 42nd AIAA Aerospace Sciences Meeting and Exhibit, 2004.

[19] D. Schafroth, S.Bouabdallah, C.Bermes, and et, al. From the test benches to the first prototype of the muFly micro helicopter. Journal of Intelligent & Robotic System, vol. 54 (1): 245-260, 2009.

[20] Y. T. Yang, C. Q.Bai, H. Y. Zhang, et al. Study on Helicopter Rotor's Dynamic Characteristics in a Combining Environment. Chinese Journal of Applied Mechanics, 03: 446-451, 2014.

[21] Z. D. Luo. Research on Vibration of Engine Cool Fan Based on Air-structure Coupling. South China University of Technology, 2012.

[22] H. J. Mohammad, G. Mostafa, Z. R. Saeed, and S. Behrooz. Dynamic Analysis of a High Speed Rotor-bearing System. Measurement, 53: 1–9, 2014.

[23] L. Li, Q. W. Guo, H. W.Song, et al. Experimental Modal Analysis and Parameter Identification of an Aluminum Plate Excited by Sound. Noise and Vibration Control, 06: 105-110. 2009.

[24] Y. F. Xu, and W. D. Zhu. Operational Modal Analysis of a Rectangular Plate Using Non-contact Excitation and Measurement. Journal of Sound and Vibration, 332: 4927-4939, 2013.

[25] R. M. V. PIDAPARTI. Structural and aerodynamic data transformation using inverse isoparametric mapping. Journal of Aircraft, 29(3): 507-509, 1992.

[26] C. B. Allen, and T. C. S. Rendall. Unified Approach to CFD-CSD Interpolation and Mesh Motion using Radial Basis Functions. In 25th AIAA Applied Aerodynamics Conference, 2007.

[27] J. M. Weiss, and W. A. Smith. Preconditioning applied to variable and constant density flows. AIAA Journal, 33: 2050-2057, 1995.

[28] Z. N. Zhou, Y. M. Li, Y. X. Gu, et al. Dynamic Characteristic Analysis of Blade Based on Fluid-Structure Coupling. Journal of China University of Mining&Technology, 38(3):120-126, 2009.